



## The sensing behavior of MgO nanotube to thiopropamine drug via DFT investigation

Farzaneh Alimohammadi <sup>1,\*</sup>, Ghasem Rezanejade Bardajee <sup>1,2</sup>, Aazam Monfared <sup>1</sup>

<sup>1</sup>Department of Chemistry, Payame Noor University, PO BOX 19395-3697, Tehran, Iran

<sup>2</sup>Department of Polymer and Materials Chemistry, Faculty of Chemistry and Petroleum Sciences, Shahid Beheshti University, 19839-63113, Tehran, Iran

### ARTICLE INFO

#### Article history:

Received 11 May 2024

Received in revised form 10 June 2024

Accepted 15 June 2024

Available online 1 August 2024

#### Keywords:

Adsorption

Conductivity

Biological

Sensor

Recovery time

### ABSTRACT

This work mainly aimed to develop a sensor based on MgO nanotubes (MgONTs) to detect thiopropamine (TP) using density functional theory (DFT). The abuse of drugs has major negative effects, and measures are to be implemented throughout the world to detect and control illegal drugs, e.g., TP. As a result, it is necessary to detect the TP drug in biological settings. The sensing characteristics of MgONTs for TP detection purposes were evaluated using DFT. MgONTs were found to have remarkable reactivity toward TP molecules and had a sensing response of 298.11. In addition, the HOMO and LUMO energy levels and therefore, the energy gap were significantly shifted by TP adsorption. The reduced energy gap was observed to raise electrical conductivity. The recovery time was short for TP desorption from the MgONT surface (nearly 18.67 ms). It can be said that MgONTs can be both efficient and effective electronic sensors of TP and a promising drug delivery system (DDS) for the TP drug in biological applications.

## 1. Introduction

It is crucial to detect and control illegal drugs since their abuse has major consequences [1-7]. The abuse of thiopropamine (TP) imposes dramatic negative effects. Hence, TP must be detected in biological settings [8-10]. Drug abuse can also lead to mental conditions [7, 11-15]. Hence, it is necessary to develop simple, affordable, and responsive sensors of significant sensitivity and accuracy to detect TP. Nanomaterials have been comprehensively used in various biological fields, such as biosensing, cell targeting, drug delivery, and bioimaging. [16-28]. The use of nanomaterials to deliver anticancer drug molecules to tumorous tissues remains a major challenge [29-33]. Nanostructured drug delivery systems (DDSs) have resulted in an intracellular treatment [34-39]. Extensive research has

been reported on the analysis of nanosheets, nanotubes, and nanoclusters in chemical sensor development in light of their major advantages over conventional sensors, including large surface-volume ratios [40-49]. Numerous studies investigated the applications of nanostructured systems consisting of elements in groups II to V. There are substantial concentrations of MgO in salt rocks. MgO possesses high chemical and thermal stability and can be employed for a wide variety of purposes, including refractory materials and catalytic agents [52,53]. MgO particles have been of significant interest to researchers. They have a large unique surface area up to 500 m<sup>2</sup>/g and the average size of their crystals is 4 nm [54]. MgO particles could be efficient adsorbents in light of their large specific surface area and great surface reactivity [55]. Researchers have experimentally [56,57] and theoretically [58-60] studied

\* Corresponding author; e-mail: [f.alimohammadi@pnu.ac.ir](mailto:f.alimohammadi@pnu.ac.ir)

<https://doi.org/10.22034/crl.2024.457011.1335>



This work is licensed under Creative Commons license CC-BY 4.0

MgO nanoclusters. Ziemann and Castleman [58] introduced the stable cubic MgO structure. Furthermore, MgO nanobelts, metal oxide nanowires, nanofilms, and nanorods have been reported [61-63]. The more recent forms of MgO include single-walled carbon nanotube (CNT)-improved MgO layers, Ga-filled MgONTs, and MgO nanotube bundles [64-66] with several potential applications. Several studies recently analyzed the constructional, electronic and adsorption properties of MgO and the interaction between MgO and single molecules [67,68]. Earlier works reported that MgONTs have a state energy of 0.12-0.66 eV (more than that of cage and cubic isomers) [69]. Valero and Yang [70] studied CO adsorption onto MgONTs. Beheshtian [71] analyzed the interaction of NO and CO molecules with the MgONT surface using DFT. They reported the strong adsorption of NO and CO gases onto MgONTs with a remarkable adsorption energy value. Peyghan et al. [72] studied N<sub>2</sub>O adsorption into MgONTs and showed that the pristine MgONT surface could not be a strong adsorbent of N<sub>2</sub>O. Ammar [73] reported the NO strong adsorption onto the MgONT surface, with an oxygen vacancy. Following the works proposing MgONT as a superb sensor for the detection of pollutants such as CO, NO, CO<sub>2</sub>, SO<sub>2</sub>, NH<sub>3</sub> and NO<sub>2</sub>, it remains yet to realize whether MgONT can be used for TP drug detection. To the best of the authors, the detection of TP molecules using MgONT adsorption systems has not been numerically studied. Therefore, the present work seeks to analyze the interaction of TP molecules with the MgONT surface to measure the potential use of MgONTs for the adsorptive sensing of TP. The sensing properties and the adsorption energy were analyzed using DFT.

## 2. Computational details

The current study executed the calculations in GAMESS [74] and carried out a density of state (DOS) analysis using GaussSum [75]. The TPSS functional is efficient for accurate electronic and structural evaluations of metal complexes [76,77]. It was employed with the 6-311G (d) basis set for the electronic, charge transfer, energetic, and structural analyses. Grimme's "D" term was also adopted for dispersion correction in the TPSS functional [76]. The counterpoise procedure has been used to obtain the basis set superposition error ( $E_{BSSE}$ ) error [78]. The adsorption energy ( $E_{ad}$ ) is written as:

$$E_{ad} = E_{(drug/MgONT)} - E_{(drug)} - E_{(MgONT)} + E_{BSSE} \quad (1)$$

where  $E_{(drug/MgONT)}$  is the TP/nanotube complex energy, while  $E_{(drug)}$  denotes the isolated drug molecule energy.

## 3. Results and discussion

A MgONT structure with a total length of 14.79 Å, five polygons, and seventy-two atoms was employed. The initial polygons showed a small planarity difference. Wilson [79] used an empirical compressible ion potential model and introduced identical and slightly distorted MgONT structures. Figure 1 shows the optimized structures and DOS plot. Two Mg–O bonds were identified, one with a length of 1.90 Å and the other one with a length of nearly 1.95 Å. The latter bond was parallel with the axis of the MgONT. However, the length of the diagonal bonds was equal to 2.03 Å by the PBE function and 2.01 Å by the TPPS function [80]. Kakkar et al. [80] reported an average Mg–O bond length of approximately 1.975 Å in the internal zone and 1.994 Å in the external zone (0.02 Å longer external bond length). It is worth mentioning that the dipole moment of the bare MgONT is 0.15 Debye. 1.23|e| charge transfer from Mg to O has been observed by the ESP charge analysis, suggesting an extremely ionic system [81].

### 3.1. Structural analysis of TP/MgONT

As be seen in Fig. 2, a TP molecule consists of 2 nucleophilic groups, i.e., S and NH<sub>2</sub>. These groups are assumed to be candidates for attacking MgONTs. The TP molecule was attached from the nucleophilic terminals to Mg atoms on the adsorbent surface. Figure 3 depicts the partial structures. This study estimated two relative minima to avoid process complication. In the most stable complex, TP molecules reacted through their N heads with an Mg atom on the adsorbent surface, with  $E_{ad} = -16.43$  kcal/mol. The N-Mg bond length was estimated to be 2.171 Å. Furthermore, there was a natural bond orbital (NBO) charge transfer as large as 0.25 |e| from the adsorbate to the adsorbent. In complex B, however, TP adsorption onto the adsorbent surface occurred through the sulfur atom, with  $E_{ad} = -5.11$  kcal/mol.

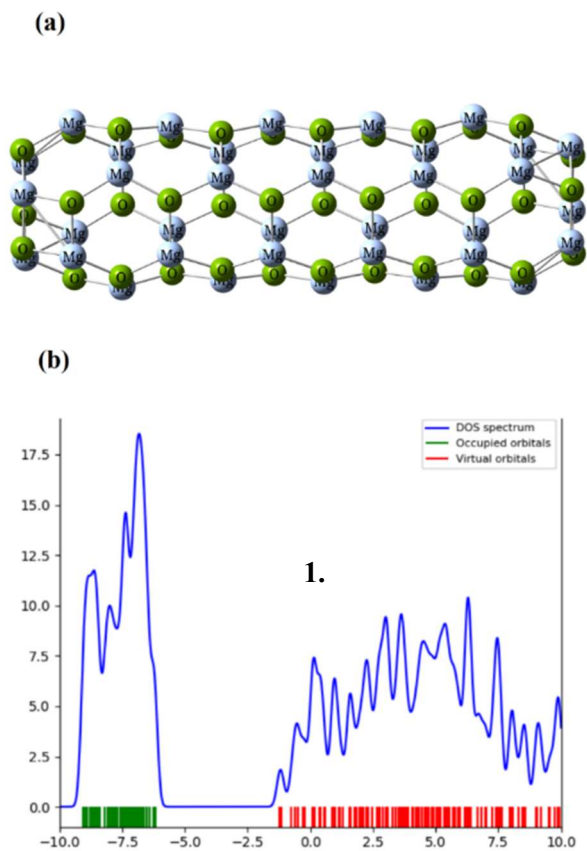


**Fig. 1.** (a) The optimized structure and (b) density of state (DOS) plot of MgONT.

Complex A had a stronger interaction than complex B. The repulsive forces between the partially positive Mg atoms of the adsorbent and the positively charged H head of the drug molecule could impose a remarkable challenge (i.e., steric hindrance) on TP adsorption. The adsorption of drug molecules onto the MgONT surface through its N atom leads to the minimization of this steric effect since N atoms carried a negative charge (pore pairs) toward Mg atoms. The single lone pair of the N atom is covered by a negative charge. When the N atom is attached to the adsorbent, the positive charge of the Mg atom is strongly attracted by the space charge of the N atom, and the steric effect is minimized. To electrically characterize the system, the net charge transfer from TP to MgONTs was analyzed in two complexes. The charge transfer to TP molecules was zero prior to the adsorption. A net charge transfer of 0.25 |e| in complex A and 0.062 |e| in complex B was measured. This implies that the direction of this charge

transfer was from the adsorbate to the adsorbent. A number of DFT studies reported different behaviors in sensor systems toward various drugs in recent years [16, 82].

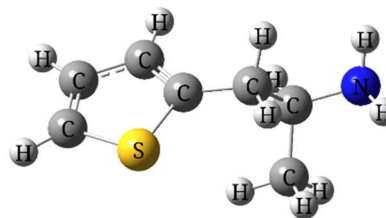


**Fig. 2.** Geometrical structure of the optimized TP drug.

### 3.2. Sensing mechanism

Resistivity variation following electron transfer between the adsorbate and adsorbent is a sensing mechanism determinant. The energy gap is related to the electronic change in MgONTs (and electrical resistance) as:

$$\sigma = AT^{3/2} \exp(-E_g / 2kT) \quad (2)$$

where A is a constant ( $e \cdot m^{-3} k^{-3/2}$ ), whereas k denotes the Boltzmann constant. As can be seen,  $\sigma$  exponentially rises for the adsorbent as the energy gap reduces. This is explained by the existence of chemical factors. The sensor response (S) is experimentally calculated as:

$$S = |R_2 - R_1| / R_1 = |(R_2 / R_1) - 1| \quad (3)$$

where  $R_1$  and  $R_2$  denote the pre- and post-adsorption electrical resistance of MgONTs, respectively. There is a reverse correlation between electrical resistance and electrical conductivity. It can be inferred that a change in electrical resistance represents adsorption-induced energy gap variation MgONTs were reported to operate at ambient temperature [83].

$$S = \left| \frac{\sigma_1}{\sigma_2} - 1 \right| = \exp(|\Delta E_g| / kT) - 1 \quad (4)$$

where  $\Delta E_g$  represents the gap energy changes after the adsorption process. According to Table 1, TP in complex A dramatically changed the LUMO, HOMO, and Fermi levels and, therefore, the energy gap pristine MgONTs were estimated to have a sensing response of 298.11 toward TP at 298 K, representing substantial sensitivity.

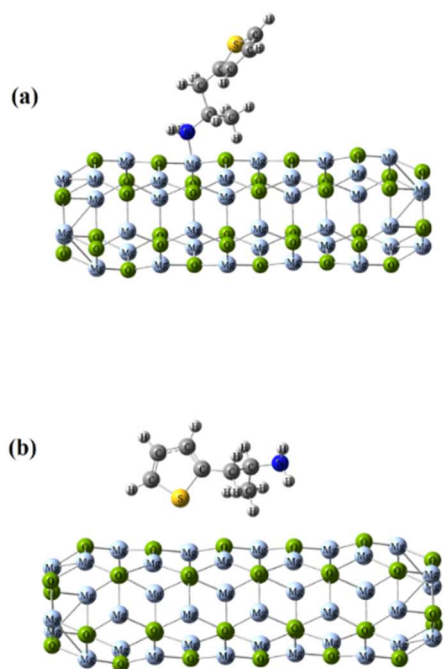


**Fig. 3.** Two various optimized structure of the MgONT/TP complexes.

### 3.3. Analysis of molecular orbitals

Figure 4 illustrates the HOMO and LUMO distributions of pristine MgONT structure and the most stable TP/MgONT structure. As can be seen, the HOMO and LUMO levels were frequently positioned near the electronegative (O and N) and electropositive (Mg) sites, respectively. The HOMO plots were mostly found on TP, whereas the LUMO levels were on MgONTs. This suggests that electrons had a higher density around O atoms. Hence, TP adsorption onto MgONTs changed the HOMO and LUMO levels (see Table 1). Furthermore, the tubular structure had the highest geometric stability obtained via 2p orbitals of O and 3s and 3p orbitals of Mg [84].

### 3.4. Recovery time

To experimentally evaluate the recovery time, the adsorbent is either heated or exposed to Ultra violet (UV) light [85]. The recovery time of TP/MgONT complexes was calculated as [86]:

$$\tau = \nu^{-1} \exp(-\Delta G/kT) \quad (5)$$

where  $\nu$  signifies the attempt frequency whereas  $k$  and  $T$  indicate the Boltzmann constant and the temperature, respectively [85-88]. For an attempt frequency of  $1018 \text{ s}^{-1}$  under UV exposure, the recovery time was obtained to be 18.67 ms at 298 K. It was found that complex A had a rapid recovery. As a result, MgONTs could be a promising sensor of TP drug.

### 3.5. Solvent effect

The effect of water as a solvent on TP adsorption onto MgONTs was measured using the polarizable continuum model (PCM) [87]. The isolated TP, pristine MgONT, and complex A were re-optimized within the solvent. It was found that the solvent slightly weakened the TP-MgONT interaction, decreasing the adsorption energy to  $-14.23 \text{ kcal/mol}$ .

Here,  $\Delta E_{ad-sol-gas}$  denotes the difference between the gaseous and aqueous adsorption energy values.

$$\Delta E_{ad-sol-gas} = E_{ad-solution} - E_{ad-gas} = 2.20 \text{ kcal/mol} \quad (6)$$

In particular, the solvation energy  $\Delta E_{solvation}$  was estimated for the isolated TP, pristine MgONTs, and TP/MgONT system as:

$$\Delta E_{solvation} = E_{solution} - E_{gas} \quad (7)$$

where  $E_{solution}$  shows the energy of the system in the aqueous medium, while  $E_{gas}$  indicates the energy of the system in the gaseous medium. The solvation energy was obtained to be  $-5.09 \text{ kcal.mol}^{-1}$  for TP,  $-7.88 \text{ kcal.mol}^{-1}$  for MgONTs, and  $-12.76 \text{ kcal.mol}^{-1}$  for the TP/MgONT system. It can be said that TP and MgONTs are highly polar and water-soluble. As a result,  $\text{H}_2\text{O}$  molecules around the MgONTs and TP molecules weaken the TP-MgONT interaction.

**Table 1.** Estimated adsorption energy ( $E_{ad}$ ) for TP drug adsorption on the MgO nanotube

Structure	$E_{ad}$ (kcal/mol)	Q (e)	D (Å)	$E_{HOMO}$ (eV)	$E_{LUMO}$ (eV)	$E_g$ (eV)	$E_F$ (eV)	$\Delta E_g$ (%)
MgONT	–	–	–	– 6.43	– 2.84	3.59	– 4.63	–
Complex A	– 16.43	0.250	2.171	– 5.20	– 2.56	2.64	– 3.88	26.46
Complex B	– 5.11	0.062	2.453	– 6.11	– 2.63	3.48	– 4.37	3.06

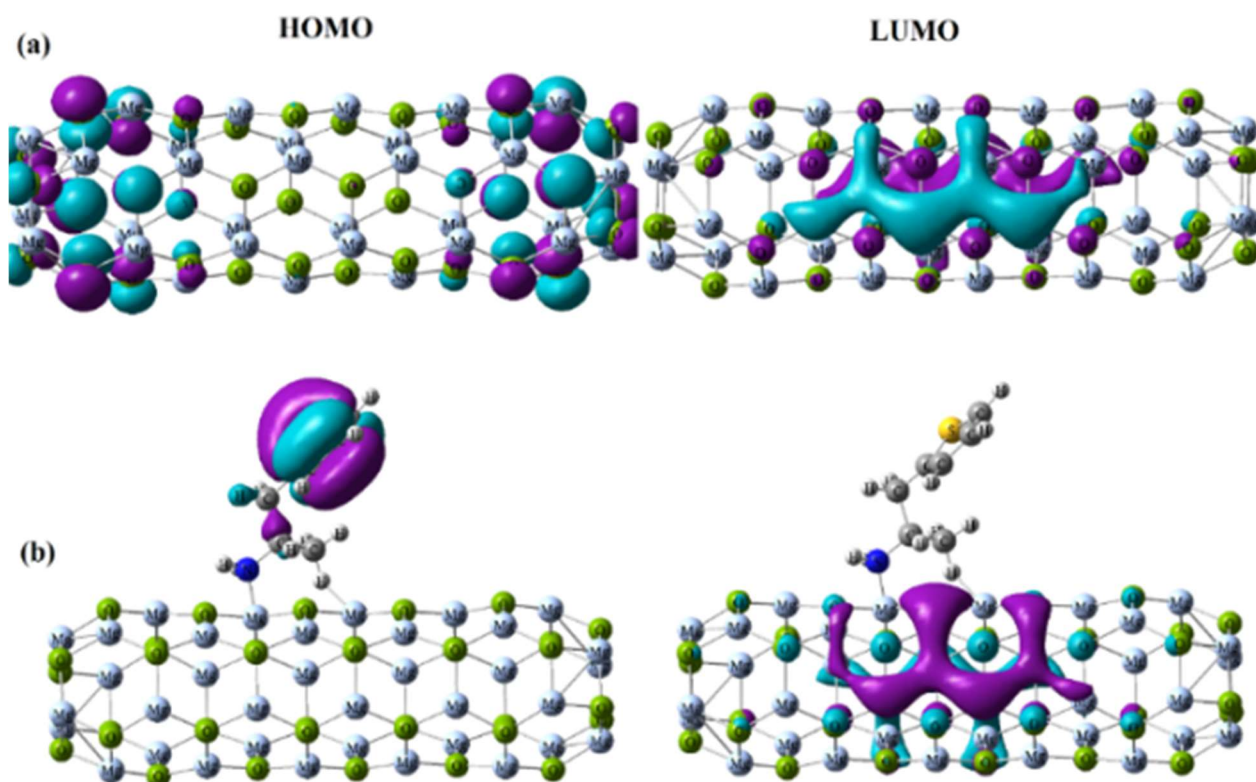


Fig. 4. The HOMO and LUMO figures of (a) MgONT and (b) most stable complex of MgONT/TP.

#### 4. Conclusion

The 1D nanostructured systems possess remarkable electronic sensitivity toward a variety of chemical agents. This study implemented DFT to analyze the potential of MgONT for the sensing of TP drug. It was found that TP would chemisorbed onto the MgONT surface ( $E_{ad} = -16.43\text{kcal/mol}$ ). The MgONT was estimated to have a sensing response of 298.11 toward TP molecules at 298 K. This is explained by the large charge transfer from TP molecules to MgONTs. In complex A, TP molecules reacted through their N heads with an Mg atom on the adsorbent surface, since Mg atoms have a small steric effect. Furthermore, MgONTs were estimated to have a rapid recovery for the desorption of TP molecules (18.67 ms). It was theoretically and numerically found that TP adsorption onto MgONTs would be modified by the electrical conductance of MgONTs. Therefore, MgONTs can be a promising biosensor of TP drug in medical settings.

#### References

- [1] K.Z. Alatawi, K.D. Albalawi, A.M. Aljuhani, N.D. Albalawi, A.I. Alalawy, A. A. Oyouni, Drug detection tests and the important factors and effects of the development of addiction, *J. King Saud Univ. Sci.* 34 (2022) 102093.
- [2] J.H. Khalsa, G. Treisman, E. McCance-Katz, E. Tedaldi, Medical consequences of drug abuse and co-occurring infections: research at the National Institute on Drug Abuse, *Nat. Lib. Med.*, 29(3) (2008) 5–16.
- [3] A.M. Nawi, R. Ismail, F. Ibrahim, M.R. Hassan, M.R. Manaf, N. Amit, N. Ibrahim, N.S. Shafuridin, Risk and protective factors of drug abuse among adolescents: *Syst. Rev.*, 21(2021) 2088.
- [4] C.T. Fakude, R.P. Modise, A.B. Haruna, J. Pillay, K.I. Ozoemena, Advances in the application of nanomaterials for the electrocatalytic detection of drugs of abuse, *Adv. Energy Mater.*, 2 (2023) 100056.
- [5] A. A. Momoh, A. Alhassan, M.O. Ibrahim, S.A. Amoo, Curtailing the spread of drug-abuse and violence comenace: An optimal control approach, *Alex. Eng. J.*, 61(6) (2022) 4399-4422.
- [6] J.E. Henningfield, M.A. Coe, R.R. Griffiths, S.J. Belouin, A. Berger, A.R. Coker, S.D. Comer, D.J. Heal, P.S. Hendricks, C.D. Nichols, F. Sapienza, F.J. Vocci,

- F.Z. Zia, Psychedelic drug abuse potential assessment research for new drug applications and Controlled Substances Act scheduling, *Neuropharmacology*, 218 (2022) 109220.
- [7] F. Baberi, D. Mirtorabi, S. Mahdavi, A. Hamed, S. Hashemi Nazari, Spatial analysis of drug abuse mortality rates in Iran, *Tox. Analyt. Cliniq.*, 35(4) (2023) 342-349
- [8] J.S. Hägele, M.G. Schmid, Enantiomeric separation of Novel Psychoactive Substances by capillary electrophoresis using (+)-18-crown-6-tetracarboxylic acid as chiral selector, *Chirality*, 30(8) (2018) 1019-1026
- [9] J.S. Hägele, M. Basrak, M.G. Schmid, Enantioselective separation of Novel Psychoactive Substances using a Lux. AMP 3  $\mu$ m column and HPLC-UV, *J. Pharm. Biomed. Anal.*, 179(5) (2020) 112967
- [10] J. Czarny, J. Musiał, J.P. Czarny, N. Galant, M. Raczkowski, B. Buszewski, R. Gadzała-Kopciuch, Validation of a simple and quick method for determination of psychoactive substances, drugs and their metabolites from human blood by LC-MS/MS, *Microchem. J.*, (2022) 182 107922
- [11] A.M. Al-Qaaneh, O.S. Al-Mohammadi, R.A. Musharraf, J.S. AlSaedi, J.L. Shaker, A.J. Aldhafiri, Prescription patterns of quetiapine for multiple drug abuse, depression, and psychosis: A retrospective study, *Saudi Pharm. J.*, 31 (2023) 101848
- [12] B. Morentin, J.J. Meana, L.F. Callado, Ethanol and illicit drugs acute use and abuse as risk factors for suicide: A case-control study based on forensic autopsies in the Basque Country, Spain, *Spanish J. Psychiatry and Mental Health*, 16 (2023) 109-115
- [13] O. Hope, O. Ness, J.G. Friesinger, A. Topor, T.D. Boe, Living needs a landscape: A qualitative study about the role of enabling landscapes for people with mental health and substance abuse problems, *Health and Place*, 84 (2023) 103144
- [14] J.M. Marraffa, Drugs of abuse. *Encyclopedia of Toxicology*, 3 (2024) 993-996.
- [15] B.L.F. Kaplan, Immunotoxicology of Drugs of Abuse, *Ref. Mod. Bio. Sci.*, (2024) <https://doi.org/10.1016/B978-0-323-95488-4.00051-6>
- [16] L. Saedi, Z. Rostami, B. Rabiei, N.O. Kattab, M. Volek, X. Hong, Identification of lomustine drug by graphyne-like, boron nitride: DFT approach, *Molecular Physics*, (2024) <https://doi.org/10.1080/00268976.2024.2318022>
- [17] H.R. Abd El-Mageed, M.A.A Ibrahim, Elucidating the adsorption and detection of amphetamine drug by pure and doped Al12N12, and Al12P12 nano-cages, a DFT study, *Mol. Phys.*, 326 (2021) 115297
- [18] X. Xu, W. Wang, J. Zhang, M. Derakhshandeh, Methylphenidate drug adsorption on the pristine magnesium oxide nanotubes; a computational study, *Comput. Theor. Chem.*, 1203 (2021) 113351
- [19] K. Hyjek, G. Kurowski, K. Dymek, A. Boguszewska-Czubara, B. Budzynska, O. Wronikowska-Denysiuk, A. Gajda, W. Piskorz, P. Sliwa, M. Szumera, P. Jelen, M. Sitarz, P. J. Jodłowski, Metal-organic frameworks for efficient mephedrone detoxification or supervised withdrawal – synthesis, characterisation, and in vivo studies, *J. Chem. Eng.*, 479 (2024) 147655
- [20] K.M. Batoo, U.A. Hussein, A. Mohammed, A. Ibrahim, B. Zazoum, N. Jamil, N. Abdulhussein, M.F. Ramadan, U.K. Radi., A. A. Ami, S. J. Al-Shuwaili, A. Elawady , X. Hong, Evaluate the potential of BC3 nanosheet in the recognition Methamphetamine drug concentration in the human body: Insights from simulation in the field of medicine, *Comput. Theor. Chem.*, 1236 (2024) 114588
- [21] Y. Yang, A. Sun, M. Eslami, A density functional theory study on detection of amphetamine drug by silicon carbide nanotubes, *Physica E Low Dimens. Syst. Nanostruct.*, 125 (2021) 114411
- [22] S. Cao, J. Huang, J. Tian, Z. Liu, H. Su, Z. Che, Deep insight into selective adsorption behavior and mechanism of novel deep eutectic solvent functionalized bio-sorbent towards methcathinone: Experiments and DFT calculation, *Environ. Res.*, 227 (2023) 115792
- [23] F. Huang, M. Liu, M. Xie, W. Liu, L. Sun, A combined study on the skeletal vibration of aminopyrine by terahertz time-domain spectroscopy and DFT simulation, *Optik.*, 208 (2020) 163913
- [24] Y. Zhang, Z. Zhang, M. A. Mustafa, S. K. Saraswat, Sh. M. Mekkey, L. Y. Qassem, M. M. Karim, A. H. Athab, Y. Elmasry, Application of biphenylene nanosheets for metronidazole detection, *J. Mol. Liq.*, 398 (2024) 124216
- [25] S.J. Hoseyni, A. Karbakhshzadeh, A. Moshtaghi Zonouz, B. Hussein, Computational investigation on interaction between graphene nanostructure BC3 and antiparkinson drug amantadine: Possible sensing study of BC3 and its doped derivatives on amantadine, *Chem Rev Lett.*, (2024) *Articles in Press*, 10.22034/CRL.2024.454413.1328
- [26] M. Azari, R. Ghiasi, B. Mirza, Binding of thymine and Molybdenocene dichloride anticancer agent: A DFT investigation, *Chem Rev Lett.*, 7(2) (2024) 286-293
- [27] A. Karbakhshzadeh, S. Majedi, V. Abbasi, Computational investigation on interaction between graphene nanostructure BC3 and Rimantadine drug: Possible sensing study of BC3 and its doped derivatives on Rimantadine, *JCHEMLETT.*, 3(2) (2022) 108-113
- [28] B. Ajdari, S. Abrahi Vahed, Fullerene (C20) as a sensing material for electrochemical detection of Nortriptyline: A theoretical study, *JCHEMLETT.*, 3(4) (2022) 164-168
- [29] J. Liu, Y. Xie, J. Ma, H. Chu, New Ca<sup>2+</sup> based anticancer nanomaterials trigger multiple cell death targeting Ca<sup>2+</sup> homeostasis for cancer therapy, *Chem Biol Interact.*, 393 (2024) 110948
- [30] Pei, Y. Yan, S. Jayaraman, P. Rajagopal, P. Natarajan, V. Umopathy, S. Gopathy, Jeane Rebecca Roy h, J. Sadagopan, D. Thalamati i, Chella P. Palanisamy, M. Mironescu k, A review on advancements in the application of starch-based nanomaterials in

- biomedicine: Precision drug delivery and cancer therapy, *Int. J. Biol. Macromol.*, 265 (2024) 130746
- [31] X. Tu, H. Xu, C. Li, X. Liu, G. Fan, W. Sun, Adsorption performance of boron nitride nanomaterials as effective drug delivery carriers for anticancer drugs based on density functional theory, *Comput. Theor. Chem.*, 1203 (2021) 113360
- [32] N. Beemkumar, M. Kaushik, A. Tripathi, M. Sharma, S. Khan, R. Sharma, Pluronic F127-chitosan modified magnesium oxide hybrid nanomaterials prepared via a one-pot method: Potential uses in antibacterial and anticancer agents, *Surf. Interfaces*, 42 (2023) 103327
- [33] M. Yousefnezhad, M. Babazadeh, S. Davaran, A. Akbarzadeh, H. Pazoki-Toroud, Preparation and in-vitro evaluation of PCL-PEG-PCL nanoparticles for doxorubicin-ezetimibe co-delivery against PC3 prostate cancer cell line, *Chem Rev Lett.*, 7(2) (2024) 159-172
- [34] M. Afshar, R. Ranjineh Khojasteh, R. Ahmadi, M. N. Moghaddam, In Silico Adsorption of Lomustin anticancer drug on the surface of Boron Nitride nanotube, *Chem Rev Lett.*, 4(3) (2021) 178-184
- [35] M. Kamel, K. Mohammadifard, Thermodynamic and reactivity descriptors Studies on the interaction of Flutamide anticancer drug with nucleobases: A computational view, *Chem Rev Lett.*, 4(1) (2021) 54-65
- [36] Z. Larian, M.H. Tabrizi, E. Karimi, N. Khatamian, G. Hosseini, H. Pourmahammadi, The folate-chitosan-decorated harmaline nanostructured lipid carrier (FCH-NLC), the efficient selective anticancer nano drug delivery system, *J Drug Deliv Sci Technol.*, 88 (2023) 104864
- [37] P. R. Avula, A.K. Chettupalli, V. Chauhan, R.K. Jadi, Design, formulation, in-vitro and in-vivo pharmacokinetic evaluation of Nicardipine-nanostructured lipid carrier for transdermal drug delivery system, *Mater. Today Chem.*, (2023) In Press, Corrected Proof, <https://doi.org/10.1016/j.matpr.2023.06.282>
- [38] S. Nurfadhlin, S. Ashari, J. Kit, N.K. Kassim, M. Hassan, N. Zainuddin, R. Mohamad, I. D. Azmi, Screening and selection of formulation components of nanostructured lipid carriers system for *Mitragyna Speciosa* (Korth). *Havil drug delivery, Ind Crops Prod.*, 198 (2023) 116668.
- [39] J. T. Mehrabad, F. Arjomandi Rad, E. Dargahi Maleki, Synthesis and characterization of Gabapentin-Zn<sub>2</sub> Al-LDH nanohybrid and investigation of its drug release and biocompatibility properties on a laboratory scale, *JCHEMLETT.*, 5(1) (2024) 71-78
- [40] S. Majedi, F. Behmagham, M. Vakili, Theoretical view on interaction between boron nitride nanostructures and some drugs, *JCHEMLETT.*, 1(1) (2020) 19-24
- [41] M. Mosavi, Adsorption behavior of mephentermine on the pristine and Si, Al, Ga-doped boron nitride nanosheets: DFT studies, *JCHEMLETT.*, 1(4) (2020) 164-171
- [42] A. Soltani, A.A. Peyghan, Z. Bagheri, H<sub>2</sub>O<sub>2</sub> adsorption on the BN and SiC nanotubes: a DFT study, *Physica E Low Dimens. Syst. Nanostruct.*, 48 (2013) 176-180
- [43] J. Beheshtian, A.A. Peyghan, Z. Bagheri, Selective function of Al<sub>12</sub>N<sub>12</sub> nano-cage towards NO and CO molecules, *Comput. Mater. Sci.*, 62 (2012) 71-74
- [44] J. Beheshtian, A.A. Peyghan, Z. Bagheri, M. Kamfiroozi, Interaction of small molecules (NO, H<sub>2</sub>, N<sub>2</sub>, and CH<sub>4</sub>) with BN nanocluster surface, *Struct. Chem.*, 23 (2012) 1567-1572
- [45] B. Adamowicz, W. Izydorczyk, J. Izydorczyk, A. Klimasek, W. Jakubik, J. Zywicki, Response to oxygen and chemical properties of SnO<sub>2</sub> thin-film gas sensors, *Vacuum*, 82 (2008) 966-970
- [46] M. Kamel, A. Morsali, H. Raissi, K. Mohammadifard, Theoretical insights into the intermolecular and mechanisms of covalent interaction of Flutamide drug with COOH and COCl functionalized carbon nanotubes: A DFT approach, *Chem Rev Lett.*, 3(1) (2020) 23-37
- [47] I. S. Hasan, A. A. Majhool, M. H. Sami, M. Adil, S. S. Abdul Azziz, DFT Investigation of structure, stability, NBO charge on Titanium-Nitrogen nanoheterofullerenes evolved from a small nanocage, *Chem Rev Lett.*, 6(3) (2023) 297-307
- [48] S. Majedi, H. Ghafur Rauf; M. Boustanbakhsh, DFT study on sensing possibility of the pristine and Al- and Ga-embedded B<sub>12</sub>N<sub>12</sub> nanostructures toward hydrazine and hydrogen peroxide and their analogues, *Chem Rev Lett.*, 24 (2019) 176-186
- [49] Mohammad Reza Jalali Sarvestani; Zohreh Doroudi, Fullerene (C<sub>20</sub>) as a potential sensor for thermal and electrochemical detection of amitriptyline: A DFT study, *JCHEMLETT.*, 1(2) (2020) 63-68
- [50] M. R. Jalali Sarvestani, S. Majedi, A DFT study on the interaction of alprazolam with fullerene (C<sub>20</sub>), *JCHEMLETT.*, 1(1) (2020) 32-38
- [51] B. Mohammadi, M. R. Jalali Sarvestani, A Comparative Computational Investigation on Amantadine Adsorption on the Surfaces of Pristine, C-, Si-, and Ga-doped Aluminum Nitride Nanosheets, *JCHEMLETT.*, 4(1) (2023) 66-70
- [52] M.A. Shand, *The chemistry and technology of magnesium*, Wiley Online, Library (2006).
- [53] M. Amft, N.V. Skorodumova, Catalytic activity of small MgO-supported Au clusters towards CO oxidation: a density functional study, *Phys. Rev.*, 81 (2010) 195443
- [54] M. Wang, Y. Chen, W. Wang, T. Zhang, Adsorption of SO<sub>2</sub> on pristine and defectivesingle-walled MgO nanotubes: a dispersion-corrected density-functional theory (DFT-D) study, *Mater. Res.*, 8 (2021) 015023
- [55] G. Xiao, R. Singh, A. Chaffee, P. Webley, Advanced adsorbents based on MgO and K<sub>2</sub>CO<sub>3</sub> for capture of CO<sub>2</sub> at elevated temperatures, *Int. J. Greenhouse Gas Control*, 5(4) (2011) 634-639
- [56] M. Yang, C. Li, Y. Zhang, D. Jia, R. Li, Y. Hou, Predictive model for minimum chip thickness and size effect in single diamond grain grinding of zirconia

- ceramics under different lubricating conditions, *Ceram. Int.*, 45 (2003) 14908–14920
- [57] W.A. Saunders, Structural dissimilarities between small II-VI compound clusters: MgO and CaO, *Phys. Rev.*, 37 (1988) 6583–6586
- [58] P.J. Ziemann, A. Castleman, Stabilities and structures of gas phase MgO clusters, *J. Chem. Phys.*, 94 (1991) 718–728
- [59] T. Gao, C. Li, D. Jia, Y. Zhang, M. Yang, Surface morphology assessment of CFRP transverse grinding using CNT nanofluid minimum quantity lubrication, *J. Clean. Prod.*, 277 (2020) 123328
- [60] M. J. Malliavin, C. Coudray, Ab initio calculations on (MgO)<sub>n</sub>, (CaO)<sub>n</sub>, and (NaCl)<sub>n</sub> clusters (n= 1–6), *J. Chem. Phys.*, 106 (1997) 2323–2330
- [61] B. Huang, L.I. Changhe, Y. Zhang, D. Wenfeng, Advances in fabrication of ceramic corundum abrasives based on sol–gel process, *Chin. J. Aeronaut.*, 34 (2021) 1–17.
- [62] R. Ma, Y. Bando, Uniform MgO nanobelts formed from in situ Mg<sub>3</sub>N<sub>2</sub> precursor, *Chem. Phys. Lett.*, 370 (2003) 770–773
- [63] Y. Yin, G. Zhang, Y. Xia, Synthesis and Characterization of MgO Nanowires Through a Vapor-Phase Precursor Method, *Adv. Funct. Mater.*, 12 (2002) 293–298
- [64] A. Szabo, C. Perri, A. Csato, G. Giordano, D. Vuono, J.B. Nagy, Synthesis Methods of Carbon Nanotubes and Related Materials, *Mater.*, 3 (2010) 3092–3140
- [65] C. Du, N. Pan, Preparation of single-walled carbon nanotube reinforced magnesium films, *Nanotechnol.*, 15 (2004) 227–231
- [66] Y.B. Li, Y. Bando, D. Golberg, Z.W. Liu, Ga-filled single-crystalline MgO nanotube: Wide-temperature range nanothermometer, *Appl. Phys. Lett.*, 83 (2003) 999–1001
- [67] J. Beheshtian, M.T. Baei, Z. Bagheri, A.A. Peyghan, Co-adsorption of CO molecules at the open ends of MgO nanotubes, *Struct. Chem.*, 23 (2012) 1981–1986
- [68] J. Beheshtian, A. Ahmadi Peyghan, Z. Bagheri, Ab initio study of NH<sub>3</sub> and H<sub>2</sub>O adsorption on pristine and Na-doped MgO nanotubes, *Struct. Chem.*, 24 (2013) 165–170
- [69] R. Dong, X. Chen, X. Wang, W. Lu, Structural transition of hexagonal tube to rocksalt for (MgO)<sub>3n</sub>, 2 ≤ n ≤ 10, *J. Chem. Phys.*, 129 (2008) 044705
- [70] R. Valero, J.R.B. Gomes, D.G. Truhlar, F. Illas, Density functional study of CO and NO adsorption on Ni-doped MgO(100), *J. Chem. Phys.*, 132 (2010) 104701
- [71] J. Beheshtian, M. Kamfiroozi, Z. Bagheri, A. Ahmadi, Computational study of CO and NO adsorption on magnesium oxide nanotubes, *Physica E-low-dimens. Syst. Nanostruct.*, 44 (2011) 546–549
- [72] A. Ahmadi Peyghan, M.T. Baei, S. Hashemian, M. Moghimi, Adsorption of nitrous oxide on the (6,0) magnesium oxide nanotube, *Chin. Chem. Lett.*, 23 (2012) 1275–1278
- [73] H. Ammar, Adsorption of NO Molecule on Oxygen Vacancy-Defected MgO Nanotubes: DFT Study, *Eur. J. Scientific Res.*, 120 (2014) 401
- [74] M. Schmidt, K. Baldrige, J. Boatz, S. Elbert, M. Gordon, J. Jenson, S. Koseki, N. Matsunaga, K. Nguyen, S.J. Su, T. Windus, M. Dupuis, J. Montgomery, General atomic and molecular electronic structure system, *J. Comp. Chem.*, 14 (1993) 1347–1363
- [75] N.M. O'Boyle, A.L. Tenderholt, K.M. Langner, cclib: a library for package-independent computational chemistry algorithms, *J. Comput. Chem.*, 29 (2008) 839–845
- [76] S. Grimme, Accurate description of van der Waals complexes by density functional theory including empirical corrections, *J. Comput. Chem.*, 25 (2004) 1463–1473
- [77] J. Tao, J.P. Perdew, V.N. Staroverov, G.E. Scuseria, Climbing the Density Functional Ladder: Nonempirical Meta-Generalized Gradient Approximation Designed for Molecules and Solids, *Phys. Rev. Lett.*, 91 (2003) 146401
- [78] S.F. Boys, F. Bernardi, The calculation of small molecular interactions by the differences of separate total energies. Some procedures with reduced errors, *Mol. Phys.*, 19 (1970) 553–566
- [79] G. Ge, Q. Jing, Y. Luo, Density functional theory study on the structural and electronic properties of Ag-adsorbed (MgO) nanoclusters, *Sci. China, Ser.*, 52 (2009) 734–741
- [80] P. Wu, G. Cao, F. Tang, M. Huang, Electronic and magnetic properties of transition metal doped MgO sheet: A density-functional study, *Comput. Mater. Sci.*, 86 (2014) 180–185
- [81] B. Badhani, N. Sharma, R. Kakkar, Gallic acid: a versatile antioxidant with promising therapeutic and industrial applications, *RSC Adv.*, 5 (2015) 27540–27557
- [82] E. Vessally, P. Farajzadeh, E. Najafi, Possible Sensing Ability of Boron Nitride Nanosheet and its Al- and Si-Doped Derivatives for Methimazole drug by Computational Study. *IJCCE*, 40 (2021) <https://doi.org/10.30492/ijcce.2021.141635.4498>
- [83] M. Nayeibzadeh, A.A. Peyghan, H. Soleymanabadi, Density functional study on the adsorption and dissociation of nitroamine over the nanosized tube of MgO, *Physica E Low Dimens. Syst. Nanostruct.*, 62 (2014) 48–54
- [84] R. Kakkar, P.N. Kapoor, K.J. Klabunde, First Principles Density Functional Study of the Adsorption and Dissociation of Carbonyl Compounds on Magnesium Oxide Nanosurfaces, *J. Phys. Chem.*, 110 (2006) 25941–25949
- [85] R. Padash, M.R. Esfahani, A.S. Rad, The computational quantum mechanical study of sulfamide drug adsorption onto X<sub>12</sub>Y<sub>12</sub> fullerene-like nanocages: detailed DFT and QTAIM investigations, *J. Biomol. Struct. Dyn.*, DOI 10.1080/07391102.2020.1792991(2020) 1-11.

- [86] A. Hosseinian, S. Soleimani-amiri, S. Arshadi, E. Vessally, L. Edjlali, Boosting the adsorption performance of BN nanosheet as an anode of Na-ion batteries: DFT studies, *Phys. Lett.*, 381 (2017) 2010–2015.
- [87] S. Sathyanarayanamoorthi, B. Suganthi, V. Kannappan, R. Kumar, Solubility study of cefpodoxime acid antibiotic in terms of free energy of solution - Insights from polarizable continuum model (PCM) analysis, *J. Mol. Liq.*, 224 (2016) 657-661
- [88] Y. Cao, Z. Rostami, R. Ahmadi, S.B. Azimi, M.M.R. Nayini, M.J. Ansari, M. Derakhshandeh, Study the role of MgONTs on adsorption and detection of carbon dioxide: First-principles density calculations, *Comput. Theor. Chem.*, 1208 (2022) 113572